Synthesis, Characterization, Biodegradation, and in Vitro Photodynamic Activities of Silicon(IV) Phthalocyanines Conjugated Axially with Poly(ε-caprolactone)

Priscilla P. S. Lee,[†] To Ngai,[†] Jian-Dong Huang,[†,‡] Chi Wu,[†,§] Wing-Ping Fong,[#] and Dennis K. P. Ng*,[†]

Department of Chemistry and Department of Biochemistry, The Chinese University of Hong Kong, Shatin, N.T., Hong Kong, China, Institute of Research on Functional Materials, Department of Chemistry, Fuzhou University, Fuzhou 350002, China, and The Open Laboratory for Bond-Selective Chemistry, Department of Chemical Physics, University of Science and Technology of China, Hefei, Anhui 230026, China

ABSTRACT: A new series of phthalocyanine-containing biodegradable poly(ε-caprolactone)s have been synthesized by ring-opening polymerization of ε-caprolactone and/or 5-ethylene ketal ε-caprolactone using silicon phthalocyanine dihydroxide as the initiator and tin(II) 2-ethylhexanoate as the catalyst. The polymers have been spectroscopically characterized, and their molecular weights have been determined by gel permeation chromatography (GPC). All the polymers exhibit typical electronic absorption and fluorescence characteristics for nonaggregated phthalocyanines. The singlet oxygen quantum yields of selected polymers have been determined and found to be slightly lower than that of unsubstituted zinc(II) phthalocyanine in *N,N*-dimethylformamide (DMF). Nanoparticles with an average hydrodynamic radius $\langle R_h \rangle$ of ∼87 nm have been prepared from the homo-poly(ε-caprolactone) **3a** and **3b** (bulk) via a microphase inversion method. The ketal-containing analogues **5**−**7** are able to form nanoparticles with a smaller dimension ($\langle R_h \rangle$ = 26−46 nm) in the absence of surfactants. The biodegradation of these systems with Lipase PS has been monitored by a combination of static and dynamic laser light scattering together with fluorescence spectroscopy, which shows that phthalocyanine rings are released during degradation. The polymers exhibit a high phototoxicity toward the HepG2 cancer cell line. The results suggest that this novel polymer-based colloidal system is potentially useful for the delivery and release of photosensitizers in photodynamic therapy.

Introduction

Being a versatile class of functional dyes, phthalocyanines have been widely studied for their applications in various disciplines.[1] Conjugation of the macrocycles with polymer chains enhances their processability and provides a means to control the molecular arrangement of the phthalocyanine rings, which is an important factor determining the properties of these materials.[2] Incorporation of poly(oxyethylene) chains to the periphery of the macrocycles, for example, induces a mesogenic behavior, promoting the formation of discotic liquid crystalline materials.[3] Polymerization of such disklike molecules with terminal alkene moieties, preorganized in a columnar manner, leads to one-dimensional polymers of phthalocyanines with high ionic and electrical conductivities.[4] Apart from the use in materials science, polymeric phthalocyanines are also highly promising for their applications in photodynamic therapy (PDT).[5] Polymeric substituents with hydrophilic character can not only enhance the solubility of the macrocycles in biological media but also prevent their aggregation, which is a prerequisite for photosensitization.[6] By controlling the size of the polymeric nanoparticles or incorporation of site-selective moieties, the biodistribu-

tion of the photosensitizers can be altered and the systems may be used for targeted delivery and release of photosensitizers. Such an approach has been extensively investigated for the delivery of various chemotherapeutic drugs.[7] However, entrapping phthalocyanines in polymeric nanoparticles for targeted PDT has been little studied.[8,9] We have recently reported a novel series of copolymers of a zinc(II) phthalocyanine and sebacic anhydride.[10] With the aid of surfactant, the copolymers form nanoparticles in water, and during degradation in an alkaline medium, phthalocyanine molecules are released. This polymer-based colloidal system is therefore potentially useful for the delivery and release of phthalocyanines in PDT. We report herein another series of polymers in which a silicon(IV) phthalocyanine core is axially linked to two biocompatible and biodegradable poly(ε-caprolactone) chains, including their preparation and characterization, together with the biodegradation and in vitro photodynamic activities of their nanoparticles formed.

Experimental Section

General. Toluene and tetrahydrofuran (THF) were distilled from sodium and sodium benzophenone ketyl, respectively. All other solvents and reagents were used as received. Silicon phthalocyanine dihydroxide (**1**)[11] and 5-ethylene ketal ε-caprolactone (**4**)[12] were synthesized by literature procedures. Lipase PS from *Pseudomonas Cepacia* (courtesy of Amano Pharmaceutical Co. Ltd., Japan) was freeze-dried prior to use.

^{1}H NMR spectra were recorded on a Bruker DPX 300 spectrometer (300 MHz) in CDCl₃ or deuterated dimethyl sulfoxide (DMSO-*d*₆). Spectra were referenced internally using

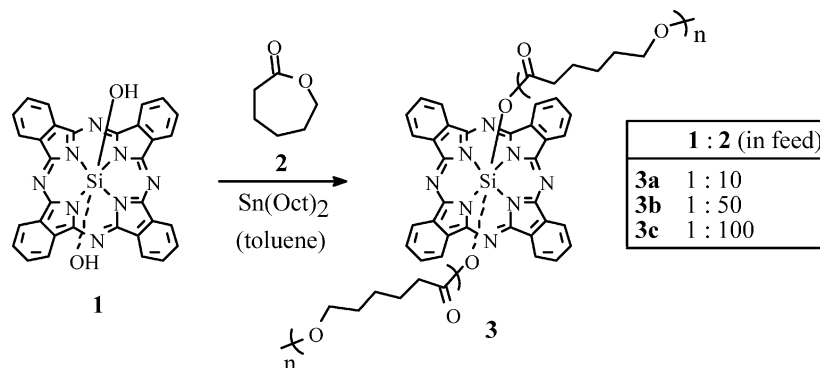* To whom correspondence should be addressed. Fax: (852) 2603 5057. E-mail: dkpn@cuhk.edu.hk.
[†] Department of Chemistry, The Chinese University of Hong Kong.
[‡] Fuzhou University.
[§] University of Science and Technology of China.
[#] Department of Biochemistry, The Chinese University of Hong Kong.

Scheme 1

	1 : 2 (in feed)
3a	1 : 10
3b	1 : 50
3c	1 : 100

the residual solvent resonances (δ 7.26 for CDCl$_3$, δ 2.49 for DMSO-d_6) relative to SiMe$_4$. UV−vis and steady-state fluorescence spectra were taken on a CARY 5G UV−vis−NIR spectrophotometer and a Hitachi F-4500 spectrofluorometer, respectively. The fluorescence quantum yields were determined by the equation $\Phi_{sample} = (F_{sample}/F_{ref})(A_{ref}/A_{sample})(n_{sample}^2/n_{ref}^2)\Phi_{ref}$, where F, A, and n are the measured fluorescence (area under the fluorescence spectra), the absorbance at 610 nm, and the refractive index of the solvent, respectively; the subscripts "sample" and "ref" denote the sample and the reference, respectively, and $\Phi_{ref} = 0.30$ for unsubstituted zinc(II) phthalocyanine (ZnPc) in 1-chloronaphthalene.[13] Singlet oxygen quantum yields (Φ_Δ) were measured by the method of chemical quenching of 1,3-diphenylisobenzofuran (DPBF) described by Wöhrle et al.,[14] except that the absolute light intensity of our system was not determined. All measurements were performed in DMF and referenced to ZnPc ($\Phi_\Delta = 0.55$).

The molecular weights and distribution for **3a**−**c** and **3a**−**c** (bulk) (the soluble portion in THF) were determined by a GPC system equipped with an ISCO 2350 pump, an ISCO V4 UV−vis absorbance detector, a Viscotek 250 viscosity/refractive index dual detector, and two Ultrastyragel columns at 35 °C. THF was used as the eluent at a flow rate of 1 mL min⁻¹. The molecular weights were calculated on the basis of polystyrene standards. For the ketal-containing polymers **5**−**7**, the data for the soluble portion in *N*-methylpyrrolidinone (NMP) were measured with a GPC system equipped with a Waters 515 HPLC pump and styragel HT 3 & 4 columns (7.8 mm × 300 mm), which were connected to a Waters 410 differential refractometer and a 996 photodiode array detector at 60 °C. NMP was used as the eluent with a flow rate of 0.8 mL min⁻¹.

Laser Light Scattering (LLS). A modified commercial LLS spectrometer (ALV/SP-125) equipped with a multi-τ digital time correlator (ALV-5000) and a solid-state diode laser (ADLAS DPY425II, output power ≈ 400 mW at $\lambda = 532$ nm) was used. In static LLS, the angular dependence of the excess absolute time-average scattered intensity, known as the Rayleigh ratio $R_{vv}(q)$, was measured. For a dilute dispersion at a relatively small scattering angle θ, $R_{vv}(q)$ can be related to the weight-average molar mass M_w, the second virial coefficient A_2, and the z-average root-mean-square radius of gyration $\langle R_g^2 \rangle_z^{1/2}$ (or simply as $\langle R_g \rangle$) by eq 1:

$$\frac{KC}{R_{VV}(q)} \approx \frac{1}{M_W}\left(1 + \frac{1}{3}\langle R_g^2 \rangle_z q^2\right) + 2A_2 C \qquad (1)$$

where $K = 4\pi^2 n^2 (\partial n/\partial C)^2/(N_A \lambda_0^4)$ and $q = (4\pi n/\lambda_0) \sin(\theta/2)$ with n, $\partial n/\partial C$, N_A, and λ_0 being the solvent refractive index, differential refractive index increment, Avogadro's number, and the wavelength of light in a vacuum, respectively. At $q \rightarrow 0$ and $C \rightarrow 0$, $R_{vv}(q) \approx KCM_w$. In dynamic LLS, the Laplace inversion of a measured intensity−intensity time correlation function $G^{(2)}(t,q)$ in the self-beating mode results in a line-width distribution $G(\Gamma)$. For a pure diffusive relaxation, $(\Gamma/q^2)_{q \rightarrow 0,c \rightarrow 0}$ is equal to the translational diffusion coefficient D, which is further related to the hydrodynamic radius R_h by the Stokes−Einstein equation: $R_h = k_B T/(6\pi\eta D)$, with k_B, T, and η being the Boltzmann constant, the absolute temperature, and the

solvent viscosity, respectively. All the measurements were carried out at 25.0 ± 0.1 °C. Details of the experimental setup and theory can be found elsewhere.[15]

Polymerization of ϵ-Caprolactone (2) or 5-Ethylene Ketal ϵ-Caprolactone (4). (A) Bulk Polymerization. A mixture of silicon phthalocyanine dihydroxide (**1**) (0.25 g, 0.44 mmol), ϵ-caprolactone (**2**) (10, 50, or 100 equiv), and tin(II) 2-ethylhexanoate (0.11 g, 0.27 mmol) was stirred under nitrogen at 100 °C overnight. After being cooled to room temperature, the mixture was diluted with THF (2 mL) and precipitated with MeOH (250 mL) via a cotton filter. The blue-green powdery polymers were collected by filtration and dried in vacuo.
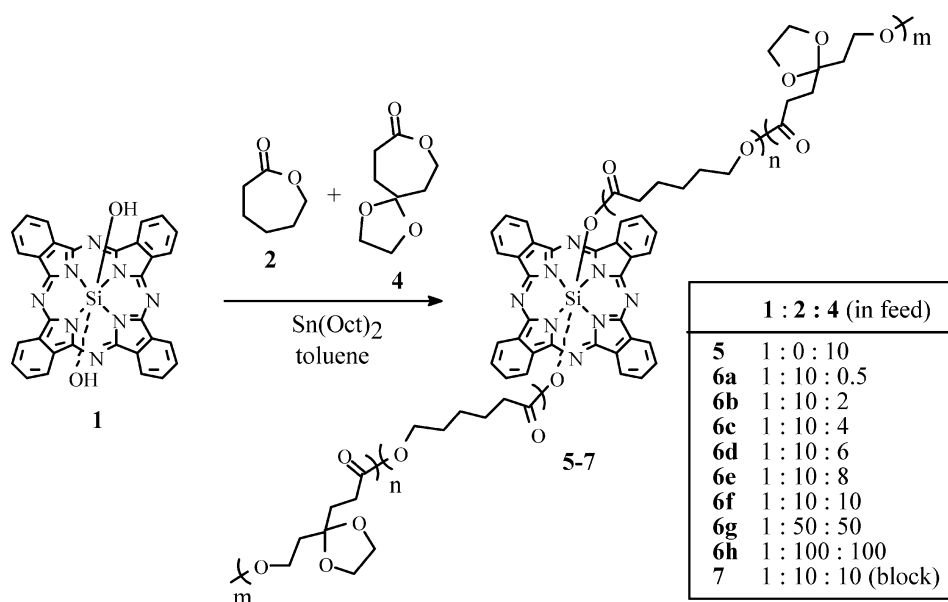
(B) Solution Polymerization. A mixture of silicon phthalocyanine dihydroxide (**1**) (0.25 g, 0.44 mmol) and tin(II) 2-ethylhexanoate (0.11 g, 0.27 mmol) in toluene (0.5 mL) was stirred at ambient temperature for 15 min under nitrogen; then ϵ-caprolactone (**2**) (10, 50, or 100 equiv with respect to **1**) or 5-ethylene ketal ϵ-caprolactone (**4**) (10 equiv with respect to **1**) in toluene (1.5 mL) was injected via a hypodermic syringe. The mixture was stirred at 100 °C overnight. After cooling, it was diluted with THF (2 mL) and precipitated with MeOH (250 mL) via a cotton filter. The polymers obtained by suction filtration were dried under reduced pressure.

Random Copolymerization of ϵ-Caprolactone (2) and 5-Ethylene Ketal ϵ-Caprolactone (4). A mixture of **1** (0.10 g, 0.17 mmol) and tin(II) 2-ethylhexanoate (0.11 g, 0.27 mmol) in toluene (0.5 mL) was stirred at ambient temperature for 15 min under nitrogen; then a mixture of ϵ-caprolactone (**2**) and 5-ethylene ketal ϵ-caprolactone (**4**) in different ratios (Scheme 2) in toluene (1.5 mL) was injected via a hypodermic syringe. The mixture was stirred at 100 °C overnight; then it was cooled and diluted with THF (2 mL). The solution was filtered via a cotton filter to MeOH (250 mL) to give a blue-green powder which was dried in vacuo.

Block Copolymerization of ϵ-Caprolactone (2) and 5-Ethylene Ketal ϵ-Caprolactone (4). A mixture of **1** (0.10 g, 0.17 mmol) and tin(II) 2-ethylhexanoate (0.11 g, 0.27 mmol) in toluene (0.5 mL) was stirred at ambient temperature for 15 min under nitrogen; then a solution of ϵ-caprolactone (**2**) (0.20 g, 1.74 mmol) in toluene (1.5 mL) was added. The mixture was stirred at 100 °C for 45 min; then a solution of 5-ethylene ketal ϵ-caprolactone (**4**) (0.30 g, 1.74 mmol) in toluene (1.0 mL) was added. The mixture was kept stirring overnight, and the resulting block copolymer **7** in blue-green powdery form was obtained as described above.

Nanoparticle Formation. Nanoparticles of polymers **3a** and **3b** (bulk) were prepared by adding dropwise a dilute solution of these polymers in THF (0.5 mL, 1.2 × 10⁻³ g mL⁻¹) into a bulk aqueous solution (50 mL) containing *n*-hexadecyltrimethylammonium bromide (CTAB) as the stabilizer, where the surfactant concentration was about twice its critical micelle concentration (cmc) (1.8 × 10⁻³ mol dm⁻³). Upon addition, the mixture was stirred vigorously. The THF diffused and mixed with water quickly. The insoluble hydrophobic polymer chains collapsed and aggregated in water to form nanoparticles which were stabilized by the surfactant molecules adsorbed on the particle surfaces. For ketal-containing polymers **5**−**7**, surfac-

Scheme 2

	1 : 2 : 4 (in feed)
5	1 : 0 : 10
6a	1 : 10 : 0.5
6b	1 : 10 : 2
6c	1 : 10 : 4
6d	1 : 10 : 6
6e	1 : 10 : 8
6f	1 : 10 : 10
6g	1 : 50 : 50
6h	1 : 100 : 100
7	1 : 10 : 10 (block)

tants were not required. To prepare nanoparticles, dilute DMF solutions (2.2×10^{-4} g mL^{-1}) of these polymers were prepared with the aid of ultrasound. The solutions (1 mL) were then mixed with deionized water (9 mL) immediately with stirring.

Biodegradation. The biodegradation was conducted in situ inside a LLS curvette. In a typical experiment, a proper amount of a dust-free Lipase PS aqueous solution was added into a 2-mL dust-free suspension of poly(ϵ-caprolactone) nanoparticles, both of which were clarified by a 0.45 μm Millipore PTFE filter. Both $R_{vv}(q)$ and $G^{(2)}(t,q)$ were simultaneously measured during the degradation. The release of phthalocyanine from the nanoparticles was monitored by absorption and fluorescence spectroscopy.

In Vitro Studies. Saturated solutions of the polymers in DMF were prepared. After passing through a 0.45 μm filter, 0.1 mL of this solution was added to an aqueous solution of Cremophor EL (Sigma) (10 mL, 0.1 mol dm^{-3}). The solution was then diluted 10 times with RPMI medium 1640 (Life Technologies) supplemented with 10% fetal calf serum (Invitrogen), and clarified with a 0.45 μm filter. Part of this stock solution was removed and adjusted to a certain concentration with the medium; then 100 μL of the resulting solution was added to the cells where the final concentration of Cremophor EL was at most 0.01 mol dm^{-3} and the DMF content was lower than 0.1% (by volume). The concentrations of the polymers were calibrated by the Q-band's absorbance in DMF.

About 2×10^4 HepG2 human hepatocarcinoma cells (ATCC) per well in the aforementioned medium were inoculated in 96-multiwell plates and incubated overnight at 37 °C under 5% CO$_2$. The cells were rinsed with phosphate buffered saline (PBS) and incubated with 100 μL of different concentrations of the polymers in the same medium for 2 h under the same conditions. The cells were then rinsed again with PBS and refed with 100 μL of the growth medium before being illuminated at ambient temperature. The light source consisted of a 300 W halogen lamp, a water tank for cooling, and a color glass filter (Newport) cut-on 610 nm. The fluence rate ($\lambda >$ 610 nm) was 40 mW cm^{-2}. An illumination of 30 min led to a total fluence of 72 J cm^{-2}.

Cell survival was determined by means of the colorimetric MTT assay.[16] After illumination, the cells were incubated at 37 °C under 5% CO$_2$ overnight. A MTT (Sigma) solution in PBS (50 μL, 3 mg mL^{-1}) was added to each well followed by incubation for 2 h under the same environment. A solution of sodium dodecyl sulfate (Sigma) in 0.04 mol dm^{-3} HCl(aq) (100 μL, 10 wt %) was then added to each well. The plate was incubated in a 60 °C oven for 30 min; then 80 μL of 2-propanol was added to each well. The plate was agitated on a Bio-Rad microplate reader at ambient temperature for 20 s before the

Table 1. Polymerization Yields, Molecular Weights, and Compositions of Poly(ϵ-caprolactone) 3 and 5−7

polymer[a]	yield (%)	$M_n{}^b$	$M_w{}^b$	PDI[b]	ratio (**2:4**)[c]
3a (bulk)	49	13000	20900	1.6	
3b (bulk)	80	21100	28900	1.4	
3c (bulk)	39	28100	96100	3.4	
3a	41	9900	12500	1.3	
3b	82	24100	46700	1.9	
3c	85	25100	52200	2.1	
5	74	6200	7400	1.2	
6a	65	6600	8300	1.3	*d*
6b	61	10100	11900	1.2	10:1.8
6c	73	11200	13600	1.2	10:3.3
6d	74	12100	13800	1.1	10:5.3
6e	57	7000	8500	1.2	10:6.5
6f	79	5200	6000	1.1	10:6.0
6g	41	5700	6700	1.2	10:7.0
6h	56	5800	6700	1.2	10:7.2
7	20	7400	8300	1.1	10:8.7

^{a} Obtained from polymerization in toluene unless otherwise stated. ^{b} Determined for the soluble portion by GPC with polystyrene standards using THF (for polymers **3**) or NMP (for polymers **5**−**7**) as the eluent. ^{c} Ratio of the two monomers (**2:4**) in the copolymers as determined by ^{1}H NMR spectroscopy. ^{d} The content of **4** was too low to be determined.

absorbance at 540 nm at each well was taken. The average absorbance of the blank wells, which did not contain the cells, was subtracted from the readings of the other wells. The cell survival was then determined by the equation cell survival (%) $= [\sum(A_i/\bar{A}_{control} \times 100)]/n$, where A_i is the absorbance of the ith data ($i = 1, 2, ..., n$), $\bar{A}_{control}$ is the average absorbance of the control wells, in which the phthalocyanine was absent, and n (≥ 3) is the number of data points.

Results and Discussion

Preparation and Characterization of Polymers. By using the readily accessible silicon phthalocyanine dihydroxide (**1**) as the initiator and tin(II) 2-ethylhexanoate [Sn(Oct)$_2$] as the catalyst,[17] ϵ-caprolactone (**2**) underwent ring-opening polymerization to give the phthalocyanine-based poly(ϵ-caprolactone) **3** (Scheme 1). The polymerization could be performed in bulk or in toluene, and the results are summarized in Table 1. Three different molar ratios of **1:2** (1:10, 1:50, and 1:100) were used. The molecular weights as determined by GPC were much higher than the theoretical values (ca.
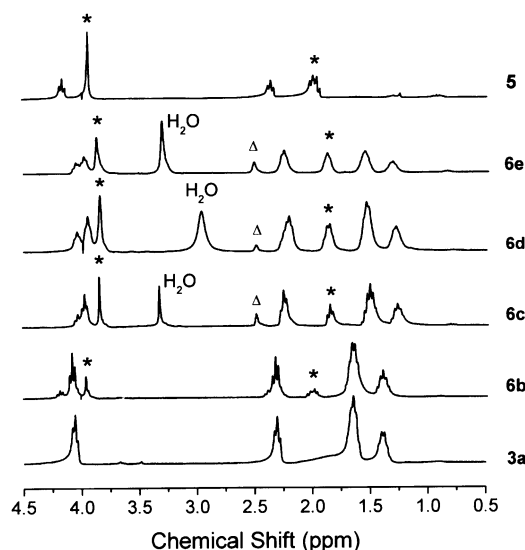
Figure 1. ^1H NMR spectra of **3a**, **5**, and **6b** in CDCl$_3$ and **6c**−**e** in DMSO-d_6; * denotes two of the signals for the poly-(5-ethylene ketal ε-caprolactone) backbone which increase in intensity as the ketal content increases; Δ indicates residual DMSO.

1700, 6300, and 12000, respectively), showing that the rate of propagation is much faster than the rate of initiation. The polydispersities (PDI) were relatively high,[17] in particular for the polymers made from a higher **1:2** ratio. The ^1H NMR spectra of **3a**−**c** in CDCl$_3$ showed the expected signals for the poly(ε-caprolactone) backbone.[18] For **3a**, two very weak signals at δ 9.67 and 8.36 also appeared for the α- and β-ring protons, respectively, of the phthalocyanine core. Some other signals at the upfield region (δ 0 to −2) were also seen in the enlarged spectrum, which could be attributed to the segment of poly(ε-caprolactone), which is situated in the shielding region of the phthalocyanine ring.

To enhance the hydrophilicity of the polymers, 5-ethylene ketal ε-caprolactone (**4**) was prepared as the other monomer. The additional ketal moiety can also allow a further functionalization.[12] This monomer could be polymerized in a similar manner to give the homopolymer **5** (Scheme 2), the molecular weight of which was significantly lower than that of the unsubstituted analogue **3a** (Table 1). A series of random copolymers **6a**−**h** were also prepared by treating phthalocyanine **1** with the monomers **2** and **4** in different ratios (Scheme 2). When a larger amount of **4** was used, the molecular weight increased initially (from **6a** to **6d**) and then decreased (from **6d** to **6f**) (Table 1). The PDI value (1.1−1.3) was significantly smaller for this series of copolymers. It seems that polymerization of **4** is slower than that of **2** so that the addition of **4** can slow the propagation rate, leading to a narrower distribution. Figure 1 shows the ^1H NMR spectra of **3a**, **6b**−**e**, and **5**, in which the ketal content is increased along the series. It can be seen that as the ketal content increases, the virtual singlet at approximately δ 4 due to the ethylene ketal protons and the multiplet at ~2 due to their neighboring methylene protons (both marked with an asterisk) become intensified compared with the other signals. The ratio of the two monomers in these copolymers could be determined from the integration, and the values are also shown in Table 1. It was found that the content of **4** for all the copolymers (except **6a**) was consistently lower than that in the feed (Scheme 2). This
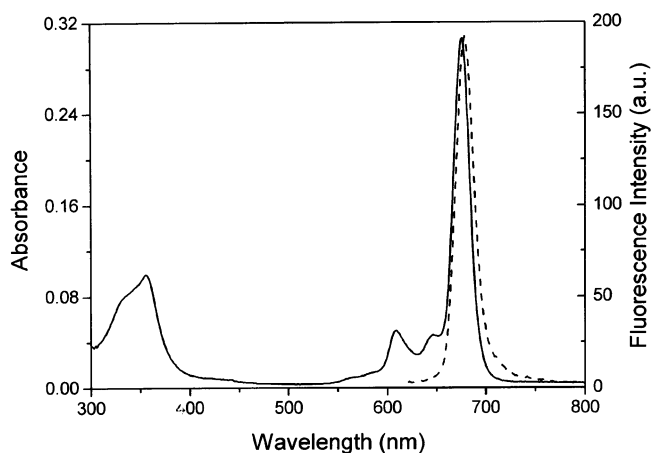
Figure 2. Electronic absorption (−) and normalized fluorescence (- - -) spectra of **3a** (bulk) in CHCl$_3$ with a concentration of 0.01 mg mL^{-1}.

**Table 2. Photophysical Data for Poly(ε-caprolactone) 3 and 5−7**

polymer	solvent	λ$_{max}$ (nm)	λ$_{em}$^{a} (nm)	Φ$_f$ ^{b}	Φ$_Δ$ ^{c}
3a (bulk)	CHCl$_3$	356, 609, 646, 676	679	0.59	0.32
3b (bulk)	CHCl$_3$	354, 610, 648, 674	679	0.62	0.35
3c (bulk)	CHCl$_3$	354, 610, 647, 678	679	0.57	0.16
3a	CHCl$_3$	357, 611, 648, 679	680	0.45	
3b	CHCl$_3$	355, 611, 649, 678	679	0.51	
3c	CHCl$_3$	336, 613, 635, 678	678	0.42	
5	THF/DMF (9/1)	355, 607, 639, 671	676	0.43	
6a	THF/DMF (9/1)	357, 607, 640, 669	673	0.30	
6b	THF/DMF (9/1)	357, 609, 648, 673	678	0.12	
6c	THF/DMF (9/1)	356, 607, 644, 675	677	0.30	0.47
6d	THF/DMF (9/1)	357, 607, 640, 671	678	0.20	
6e	THF/DMF (9/1)	355, 607, 638, 671	673	0.10	
6f	THF/DMF (9/1)	355, 607, 642, 670	676	0.33	0.44
6g	THF/DMF (9/1)	354, 607, 641, 670	677	0.35	
6h	THF/DMF (9/1)	354, 607, 641, 671	674	0.29	
7	CHCl$_3$/DMF (9/1)	356, 611, 649, 678	683	0.06	

^{a} Excited at 610 nm. ^{b} Relative to ZnPc (Φ$_f$ = 0.30 in 1-chloronaphthalene). ^{c} Measured in DMF and relative to ZnPc (Φ$_Δ$ = 0.55 in DMF).

again showed that polymerization of **4** proceeds less readily than that of **2**.

Apart from the random copolymers of **2** and **4**, a phthalocyanine-containing block copolymer of these monomers was also prepared. By sequential addition of **2** and then **4** to a mixture of **1** and Sn(Oct)$_2$ in toluene, copolymer **7** was obtained in 20% yield which was also characterized with ^1H NMR spectroscopy and GPC measurements (Scheme 2 and Table 1).

Photophysical Properties. All the polymers exhibited electronic absorptions which are typical for non-aggregated phthalocyanines. Figure 2 shows the absorption spectrum of **3a** (bulk) in CHCl$_3$ for exemplification. The spectrum shows a strong and sharp Q-band at 676 nm together with a B (or Soret) band at 356 nm and two weak vibronic bands at 609 and 646 nm. These values do not change significantly for the whole series of polymers (Table 2), showing that the length and the nature of the polymeric substituents do not significantly perturb the π system. Upon excitation at 610 nm, these polymers showed a fluorescence emission with a Stokes shift of 0−7 nm. The fluorescence quantum yield (Φ$_f$) was generally higher for the homopolymers **3a**−**c** (Table 2). A normalized fluorescence spectrum of **3a** (bulk) in CHCl$_3$ is also shown in Figure 2.
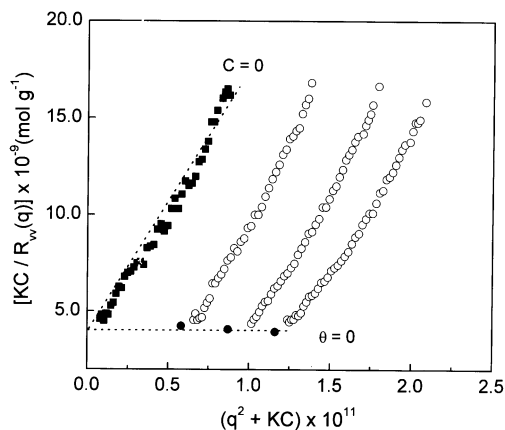
Figure 3. Typical Zimm plot for the nanoparticles of **3b** (bulk) in the presence of CTAB (2(cmc)) at 25 °C, where the concentration of **3b** (bulk) ranges from 5.8×10^{-6} to 1.2×10^{-5} g mL^{-1}.

To evaluate the photosensitizing efficiency of these phthalocyanines entrapped with two polymer chains, the singlet oxygen quantum yields (Φ_Δ) of **3a−c** (bulk), **6c**, and **6f** were determined by a steady-state method using 1,3-diphenylisobenzofuran (DPBF) as the scavenger. The concentration of the quencher was monitored spectroscopically at 411 nm along with time, from which the values of Φ_Δ could be determined.[14] It was found that all these polymers are singlet oxgen generators, but the values of Φ_Δ, as shown in Table 2, are slightly lower than that of ZnPc ($\Phi_\Delta = 0.55$), which was used as the standard.

Nanoparticle Formation and Biodegradation. Micronization of **3b** (bulk) was performed by adding dropwise a dilute THF solution of **3b** (bulk) into a large amount of aqueous solution containing CTAB at twice the cmc. The final concentration of **3b** (bulk) was 1.2×10^{-5} g mL^{-1}, and the average hydrodynamic radius $\langle R_h \rangle$ of the resulting nanoparticles was 87 nm, as determined by dynamic laser light scattering. Figure 3 shows a typical Zimm plot for the CTAB-stabilized nanoparticles of **3b** (bulk) in water, which incorporates the angular and concentration dependence of the Rayleigh ratio $R_{vv}(q)$ on a single grid. According to eq 1, the extrapolation of $[KC/R_{vv}(q)]$ to $C \rightarrow 0$ and $q \rightarrow 0$ leads to the value of M_w (2.35×10^8 g mol^{-1}), while the slopes for the lines plotting $[KC/R_{vv}(q)]_{C\rightarrow0}$ vs q^2 and $[KC/R_{vv}(q)]_{q\rightarrow0}$ vs C give the values of $\langle R_g \rangle$ (69 nm) and A_2 (≈ 0), respectively. From the values of M_w and $\langle R_h \rangle$, the average particle density $\langle \rho \rangle$ was estimated to be 0.14 g mL^{-1}. The low value suggests that the nanoparticles are composed of loosely aggregated polymer chains with a large number of water molecules trapped inside. The ratio $\langle R_g \rangle / \langle R_h \rangle$ was found to be 0.79, which is close to the value of 0.774 predicted for a uniform sphere, suggesting that the nanoparticles are spherical and uniform.[19]

Polymer **3a** was also micronized using the same procedure. The resulting nanoparticles were subjected to biodegradation with Lipase PS.[20] On the basis of eq 1, at $C \rightarrow 0$ and $q \rightarrow 0$, the ratio $[R_{vv}(q)]_t/[R_{vv}(q)]_0$ is proportional to $[CM_w]_t/[CM_w]_0$, where the subscripts "t" and "0" denote the quantities at time t and the initial values, respectively. Therefore, a decrease in $[R_{vv}(q)]_t/[R_{vv}(q)]_0$ could be related to a decrease in M_w and/or C. Figure 4 shows the variation of this ratio and $\langle R_h \rangle$ with degradation with Lipase PS. It can be seen that the value of $\langle R_h \rangle$ remains relatively unchanged, implying a relatively constant molar mass distribution. The de-
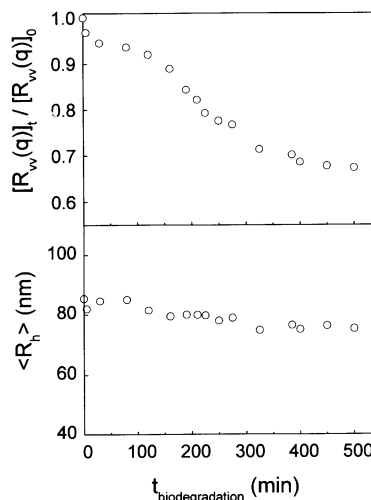
Figure 4. Biodegradation time dependence of the relative Rayleigh ratio $[R_{vv}(q)]_t/[R_{vv}(q)]_0$ and the average hydrodynamic radius $\langle R_h \rangle$ of the CTAB-stabilized nanoparticles of **3a** at 25 °C, where the initial concentration of **3a** (C_0) = 1.2×10^{-5} g mL^{-1} and the concentration of Lipase PS = 3.1×10^{-4} g mL^{-1}.
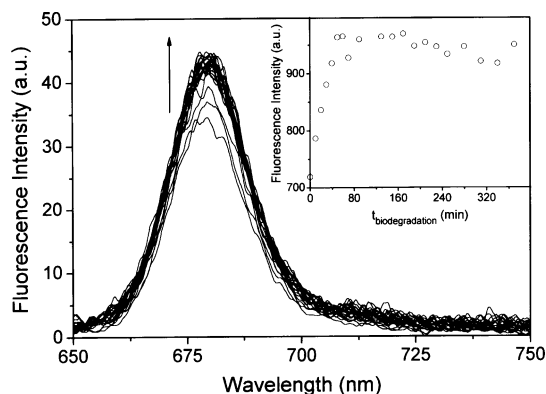

Figure 5. Change in the fluorescence spectrum of CTAB-stabilized nanoparticles of **3a** during biodegradation with Lipase PS at 25 °C, where $C_0 = 1.2 \times 10^{-5}$ g mL^{-1} and the concentration of Lipase PS = 3.1×10^{-4} g mL^{-1}. The inset shows the degradation time dependence of the fluorescence intensity.

crease in $[R_{vv}(q)]_t/[R_{vv}(q)]_0$ is thus due to the decrease in C_t/C_0 or simply the number of the nanoparticles.

The degradation was also followed by fluorescence spectroscopy. As shown in Figure 5, the fluorescence emission due to the phthalocyanine core increases during the initial stage of degradation and then reaches a steady value. It is likely that, due to the collapse of polymer chains during the formation of nanoparticles in water, the phthalocyanine rings are somewhat aggregated. A partial scissoring of the polymer chains upon degradation releases some phthalocyanine-containing fragments, in which the residual axial substituents together with the broken poly(ϵ-caprolactone) chains and the surfactant CTAB reduce the aggregation of phthalocyanine, leading to a higher fluorescence intensity.[21] However, compared with the case of the zinc analogue conjugated with poly(sebacic anhydride),[10] the increase in fluorescence intensity is less substantial. This can be attributed to the additional axial substituents in the present case which are rather effective to prevent stacking of the molecules.

Polymers **6** and **7**, which contain ketal moieties, were able to form nanoparticles in the absence of surfactants. The average hydrodynamic radius $\langle R_h \rangle$ ranged from 26
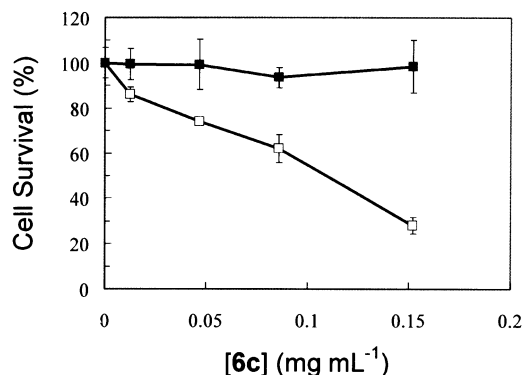
Figure 6. Dark-toxicity (■) and phototoxicity (□) of **6c** toward HepG2. For the latter, the cells were illuminated with a red light ($\lambda > 610$ nm, 40 mW cm^{-2}, 72 J cm^{-2}). Values are expressed as mean $\pm$ SD ($n \geq 3$).

to 46 nm, and there seemed to be no correlation with the ketal content. The surfactant-free nanoparticles of **6f** were subjected to biodegradation using Lipase PS again. Without the protection of the surfactant molecules, the rate of degradation was much faster than that for the CTAB-stabilized nanoparticles of **3a**; only 10 min was required to reach a steady value of $[R_{vv}(q)]_t/[R_{vv}(q)]_0$. While a rather broad Q-band at 678 nm was observed for the nanoparticles in water, which slightly decreased in intensity during degradation, surprisingly, the system did not fluoresce. Presumably, in the absence of surfactant, the phthalocyanine rings become highly aggregated in the nanoparticles, thereby enhancing the nonradiative relaxation pathway.[21]

In Vitro Photodynamic Activities. The phototoxicity of polymers **3a**, **5**, **6a**−**e**, and **7** toward HepG2 human hepatocarcinoma cells was examined. In an initial screening where the cells were incubated with about the same concentration of the polymers (ca. 0.05 mg mL^{-1}) formulated with Cremophor EL, all the polymers were found to be essentially nontoxic in the dark. Upon illumination with a red light ($\lambda > 610$ nm, total fluence = 72 J cm^{-2}), polymer **6c** exhibited the highest photodynamic activity with a cell viability of about 70%, while the other polymers could only attain 85−97%. The reasons for the slightly higher photodynamic activity of **6c** remained unclear at this stage. Nevertheless, the dosage−activity relationship of this polymer was further investigated. Figure 6 shows the survival curve for HepG2 using **6c** as the photosensitizer. It can be seen that the phototoxicity increases with the concentration of **6c**. The cell viability drops to 28% when the concentration of the polymer increases by 3-fold (ca. 0.15 mg mL^{-1}). Since the actual content of silicon phthalocyanine in this copolymer is only about 4%, if one considers the high molecular weight of this polymer ($M_w \approx 13\ 600$), the concentration of the phthalocyanine photosensitizer is in fact very low ($\approx 10\ \mu$mol dm^{-3}), indicating the high photodynamic activity of this polymeric system.

Conclusion

We have prepared a novel series of phthalocyanine-containing biodegradable poly(ϵ-caprolactone)s and micronized some of these polymers into nanoparticles via a microphase inversion method. Surfactant-free nanoparticles can be formed for those which are functionalized with ethylene ketal moieties. The degradation of

these nanoparticles and the release of phthalocyanine have been monitored with a combination of laser light scattering and fluorescence spectroscopy. A preliminary in vitro study has shown that these polymers exhibit a high photodynamic activity toward HepG2 cells. The results show that this biocompatible polymer-based colloidal system is potentially useful for the delivery and release of photosensitizers in PDT.

References and Notes

(1) (a) *Phthalocyanines—Properties and Applications*; Leznoff, C. C., Lever, A. B. P., Eds.; VCH: New York, 1989; Vol. 1, 1993; Vols. 2 and 3, 1996; Vol. 4. (b) McKeown, N. B. *Phthalocyanine Materials: Synthesis, Structure and Function*; Cambridge University Press: Cambridge, 1998.

(2) (a) McKeown, N. B. *J. Mater. Chem.* **2000**, *10*, 1979. (b) Wöhrle, D. *Macromol. Rapid Commun.* **2001**, *22*, 68.

(3) (a) Clarkson, G. J.; Cook, A.; McKeown, N. B.; Treacher, K. E.; Ali-Adib, Z. *Macromolecules* **1996**, *29*, 913. (b) Toupance, T.; Bassoul, P.; Mineau, L.; Simon, J. *J. Phys. Chem.* **1996**, *100*, 11704.

(4) (a) van der Pol, J. F.; Neeleman, E.; van Miltenburg, J. C.; Zwikker, J. W.; Nolte, R. J. M.; Drenth, W. *Macromolecules* **1990**, *23*, 155. (b) Drager, A. S.; Zangmeister, R. A. P.; Armstrong, N. R.; O'Brien, D. F. *J. Am. Chem. Soc.* **2001**, *123*, 3595.

(5) (a) Gu, Z.-W.; Spikes, J. D.; Kopecková, P.; Kopecek, J. *Collect. Czech. Chem. Commun.* **1993**, *58*, 2321. (b) Foley, S.; Jones, G.; Liuzzi, R.; McGarvey, D. J.; Perry, M. H.; Truscott, T. G. *J. Chem. Soc., Perkin Trans. 2* **1997**, 1725. (c) Brasseur, N.; Ouellet, R.; La Madeleine, C.; van Lier, J. E. *Br. J. Cancer* **1999**, *80*, 1533. (d) Lo, P.-C.; Wang, S.; Zeug, A.; Meyer, M.; Röder, B.; Ng, D. K. P. *Tetrahedron Lett.* **2003**, *44*, 1967.

(6) (a) Dhami, S.; Phillips, D. *J. Photochem. Photobiol., A: Chem.* **1996**, *100*, 77. (b) Howe, L.; Zhang, J. Z. *J. Phys. Chem. A* **1997**, *101*, 3207. (c) Fernández, D. A.; Awruch, J.; Dicelio, L. E. *J. Photochem. Photobiol., B: Biol.* **1997**, *41*, 227. (d) Lang, K.; Kubát, P.; Mosinger, J.; Wagnerová, D. M. *J. Photochem. Photobiol., A: Chem.* **1998**, *119*, 47.

(7) See, for example: (a) Kim, J. H.; Emoto, K.; Iijima, M.; Nagasaki, Y.; Aoyagi, T.; Okano, T.; Sakurai, Y.; Kataoka, K. *Polym. Adv. Technol.* **1999**, *10*, 647. (b) Nishiyama, N.; Yokoyama, M.; Aoyagi, T.; Okano, T.; Sakurai, Y.; Kataoka, K. *Langmuir* **1999**, *15*, 377. (c) Yokoyama, M.; Okano, T.; Sakurai, Y.; Fukushima, S.; Okamoto, K.; Kataoka, K. *J. Drug Targeting* **1999**, *7*, 171. (d) Kataoka, K.; Matsumoto, T.; Yokoyama, M.; Okano, T.; Sakurai, Y.; Fukushima, S.; Okamoto, K.; Kwon, G. S. *J. Controlled Release* **2000**, *64*, 143. (e) Jung, T.; Kamm, W.; Breitenbach, A.; Kaiserling, E.; Xiao, J. X.; Kissel, T. *Eur. J. Pharm. Biopharm.* **2000**, *50*, 147. (f) Wang, D.; Kopecková, P.; Minko, T.; Nanayakkara, V.; Kopecek, J. *Biomacromolecules* **2000**, *1*, 313.

(8) (a) Labib, A.; Lenaerts, V.; Chouinard, F.; Leroux, J. C.; Ouellet, R.; van Lier, J. E. *Pharm. Res.* **1991**, *8*, 1027. (b) Allemann, E.; Rousseau, J.; Brasseur, N.; Kudrevich, S. V.; Lewis, K.; van Lier, J. E. *Int. J. Cancer* **1996**, *66*, 821. (c) Leroux, J. C.; Allemann, E.; DeJaeghere, F.; Doelker, E.; Gurny, R. *J. Controlled Release* **1996**, *39*, 339. (d) Taillefer, J.; Jones, M.-C.; Brasseur, N.; van Lier, J. E.; Leroux, J.-C. *J. Pharm. Sci.* **2000**, *89*, 52. (e) Taillefer, J.; Brasseur, N.; van Lier, J. E.; Lenaerts, V.; Le Garrec, D.; Leroux, J.-C. *J. Pharm. Pharmacol.* **2001**, *53*, 155. (f) Le Garrec, D.; Taillefer, J.; van Lier, J. E.; Lenaerts, V.; Leroux, J.-C. *J. Drug Targeting* **2002**, *10*, 429.

(9) (a) Chowdhary, R. K.; Dolphin, D. H. *PCT Int. Appl.* WO 01 85,212 (*Chem. Abstr.* **2001**, *135*, 376748g). (b) Chen, J. *U. S. Pat. Appl. Publ.* US 2002 127,224 (*Chem. Abstr.* **2002**, *137*, 206638v).

(10) Fu, J.; Li, X.-y.; Ng, D. K. P.; Wu, C. *Langmuir* **2002**, *18*, 3843.

(11) Davison, J. B.; Wynne, K. J. *Macromolecules* **1978**, *11*, 186.

(12) Tian, D.; Dubois, P.; Grandfils, C.; Jérome, R. *Macromolecules* **1997**, *30*, 406.

(13) Ferraudi, G. In *Phthalocyanines—Properties and Applications*; Leznoff, C. C., Lever, A. B. P., Eds.; VCH: New York, 1989; Vol. 1, p 301.

(14) Spiller, W.; Kliesch, H.; Wöhrle, D.; Hackbarth, S.; Röder, B.; Schnurpfeil, G. *J. Porphyrins Phthalocyanines* **1998**, *2*, 145.

(15) (a) Berne, B.; Pecora, R. *Dynamic Light Scattering*; Plenum Press: New York, 1976. (b) Chu, B. *Laser Light Scattering*, 2nd ed.; Academic Press: New York, 1991. (c) Wu, C.; Zhou, S. Q. *Macromolecules* **1995**, *28*, 8381. (d) Wu, C.; Zhou, S. Q. *Macromolecules* **1996**, *29*, 1574.

(16) MTT = 3-(4,5-dimethyl-2-thiazolyl)-2,5-diphenyl-2*H*-tetrazolium bromide. Tada, H.; Shiho, O.; Kuroshima, K.; Koyama, M.; Tsukamoto, K. *J. Immunol. Methods* **1986**, *93*, 157.

(17) (a) Trollsås, M.; Lee, V. Y.; Mecerreyes, D.; Löwenhielm, P.; Möller, M.; Miller, R. D.; Hedrick, J. L. *Macromolecules* **2000**, *33*, 4619. (b) Hecht, S.; Vladimirov, N.; Fréchet, J. M. J. *J. Am. Chem. Soc.* **2001**, *123*, 18. (c) Dong, C.-M.; Qiu, K.-Y.; Gu, Z.-W.; Feng, X.-D. *Macromolecules* **2001**, *34*, 4691.

(18) Shibasaki, Y.; Sanada, H.; Yokoi, M.; Sanda, F.; Endo, T. *Macromolecules* **2000**, *33*, 4316.

(19) Tu, Y.; Wan, X.; Zhang, D.; Zhou, Q.; Wu, C. *J. Am. Chem. Soc.* **2000**, *122*, 10201.

(20) (a) Gan, Z.; Fung, J. T.; Jing, X.; Wu, C.; Kuliche, W.-K. *Polymer* **1999**, *40*, 1961. (b) Gan, Z.; Jim, T. F.; Li, M.; Yuer, Z.; Wang, S.; Wu, C. *Macromolecules* **1999**, *32*, 590.

(21) Ng, A. C. H.; Li, X.-y.; Ng, D. K. P. *Macromolecules* **1999**, *32*, 5292.